Organosulfate Produced from Consumption of SO3 Speeds up Sulfuric Acid-Dimethylamine Atmospheric Nucleation

Xiaomeng Zhang[a], *Yongjian Lian*[a], *Shendong Tan*[a] *and Shi Yin*[*a]

[a] MOE & Guangdong Province Key Laboratory of Laser Life Science & Institute of Laser Life Science, Guangzhou Key Laboratory of Spectral Analysis and Functional Probes, College of Biophotonics, South China Normal University, Guangzhou 510631, P. R. China

AUTHOR INFORMATION

Corresponding Author

*Shi Yin, E-mail: yinshi@m.scnu.edu.cn

Supporting information

Table of contents

The concentration of glycolic acid sulfate (GAS) and glycolic acid sulfuric anhydride (GASA)

The formation of GAS and GASA can be described by following two reactions, respectively.

$$(GA + SO_3)_{-OH} \rightarrow GAS$$

$$(GA + SO_3)_{-COOH} \rightarrow GASA$$

The equilibrium constant $K_{(GA + SO3)-OH}$ for the formation of GAS and $K_{(GA + SO3)-COOH}$ for the formation of GASA are

$$K_{(GA + SO3)-OH} = \frac{[GAS]}{[GA][SO_3]} = e^{\frac{-\Delta G}{RT}}$$

$$K_{(GA + SO3)-COOH} = \frac{[GASA]}{[GA][SO_3]} = e^{\frac{-\Delta G}{RT}}$$

And the equilibrium concentration of GAS and GASA can be roughly estimated theoretically using the following expressions:

$$[GAS] = K_{(GA + SO3)-OH}\,[GA][SO_3]$$

$$[GASA] = K_{(GA + SO3)-COOH}\,[GA][SO_3]$$

where $K_{(GA + SO3)-OH}$ and $K_{(GA + SO3)-COOH}$ are equal to the equilibrium constants from the formation Gibbs energies of the GAS and GASA, respectively. [GA] and [SO_3] are the concentration of GA and SO_3 monomer, respectively. We use the reactant concentrations of [GA] = 1.11×10^7-2.72×10^9 molecules cm^{-3}, [SO_3] = 10^5 molecules cm^{-3} according to the values of some field observations[1-4]. Based on the above equations, the estimated concentration of the reaction product, GAS, is about 2.14×10^3-5.24×10^5 molecules cm^{-3}, and GASA is about 2.30×10^{-6}-5.62×10^{-4} molecules cm^{-3}. Thus, a range of concentration for GAS, from 10^3 to 10^5 molecules cm^{-3} as shown in Table S1, is selected for the discussion in this work.

Selection of simulated box and boundary clusters

For H_2SO_4-DMA system, "3 × 3" box has always been adopted in previous studies[5]. The box for the H_2SO_4-DMA-based system is set to the size of "3 × 3" to contain the **$(GA)_x(SA)_y(DMA)_z$, $(GAS)_x(SA)_y(DMA)_z$, and $(GAS)_x(SA)_y(DMA)_z$ ($0 \le z \le x + y \le 3$) clusters.**

In the process of cluster growth, the stability of cluster can be judged by the competition between evaporation into smaller clusters or collision. The collision rate constant of a cluster with acid or base monomer is of the order of 10^{-10} cm^3 s^{-1}, and the collision rate can be considered to be about 10^{-2} s^{-1} under the condition of base/acid monomers at ppt level. Thus, the cluster can be considered to be stable enough when the collision rate is higher than that of evaporation, and a given cluster can be deemed as stable enough for further growth when the evaporation rate is lower than 10^{-3} s^{-1}.

The boundary clusters are allowed to leave the simulation box for further growth, which means the boundary clusters are needed to be stable enough and have the potential to continue growing. Furthermore, generally speaking, the clusters with approximately equal numbers of acidic molecules and base molecules or number of acidic molecules one greater than that of base molecules are assumed to have the potential for further growth. Hence, only clusters that satisfy the above conditions are calculated.

As shown in Figure S3, the evaporation rates for all glycolic acid (GA)-involved clusters has been predicted to be higher than 10^1 s^{-1}. Therefore, the boundary clusters are $(SA)_4(SA)_3$ and $(SA)_4(SA)_4$ clusters for GA-SA-DMA system. As for GAS-SA-DMA system, the $(GAS)_3(DMA)_3$, $(GAS)_2(DMA)_2$, and $(GAS)_1(SA)_2(DMA)_3$ clusters are stable enough against evaporation. Thus, $(GAS)_4(DMA)_3$, $(GAS)_4(DMA)_4$, $(GAS)_2(SA)_2(DMA)_3$, $(GAS)_2(SA)_2(DMA)_4$, $(GAS)_3(SA)_1(DMA)_3$, $(GAS)_3(SA)_1(DMA)_4$, $(GAS)_1(SA)_3(DMA)_3$, $(GAS)_1(SA)_3(DMA)_4$, $(SA)_4(SA)_3$ and $(SA)_4(SA)_4$ clusters are acting as boundary clusters for GSA-SA-DMA system. Similarly, the $(GASA)_4(DMA)_3$, $(GASA)_4(DMA)_4$, $(GASA)_2(SA)_2(DMA)_3$, $(GASA)_2(SA)_2(DMA)_4$, $(GASA)_3(SA)_1(DMA)_3$, $(GASA)_3(SA)_1(DMA)_4$, $(GASA)_1(SA)_3(DMA)_3$, $(GASA)_1(SA)_3(DMA)_4$, $(SA)_4(SA)_3$ and $(SA)_4(SA)_4$ clusters are defined as boundary clusters for GASA-SA-DMA system for the reason that $(GASA)_3(DMA)_3$, $(GASA)_2(DMA)_2$, and $(GASA)_1(SA)_2(DMA)_3$ clusters are stable enough against evaporation.

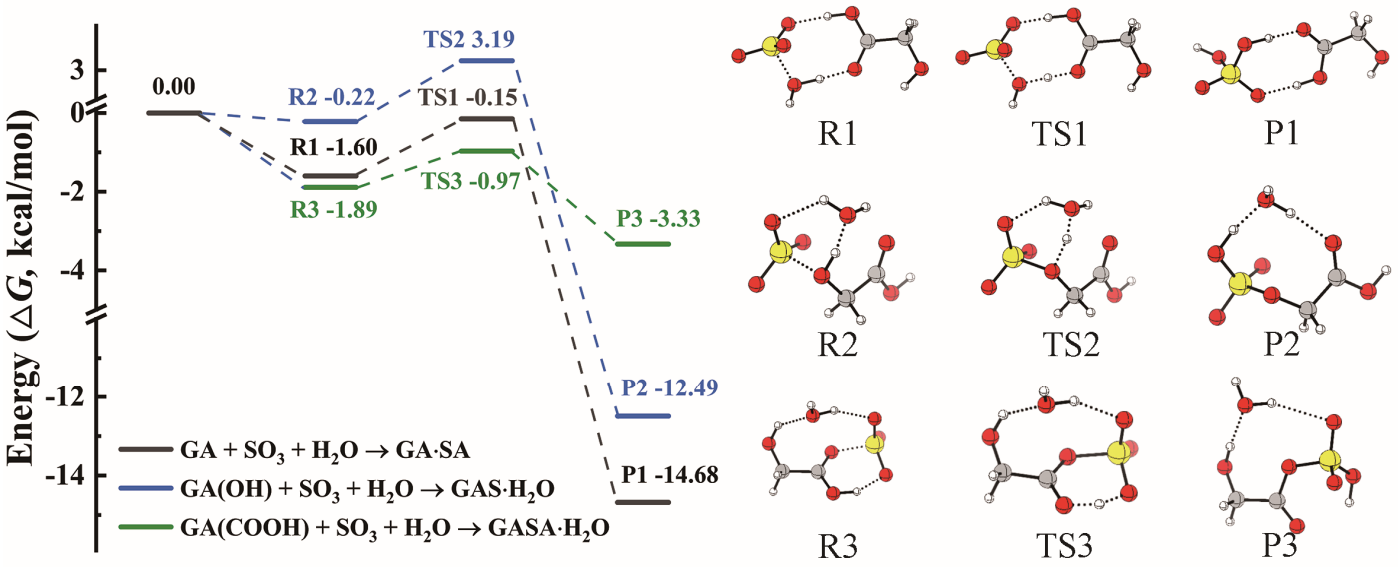

Figure S1. Potential energy surfaces at the DLPNO-CCSD(T)/aug-cc-pVTZ//M06-2X/6-311++G(3df,3pd) level of theory in units of kcal mol^{-1} (at 298 K, 1atm) for the gas-phase reaction of GA, SO_3 and H_2O. The red line represents the pathway through SO_3 attacking the -OH group of GA with H_2O as a catalyst; the blue one represents the SO_3 attacking the -COOH group of GA pathway with H_2O as a catalyst; and black one represents the pathway to form H_2SO_4 with as a catalyst. R, TS, and P refer to pre-reaction complex, transition state, and product, respectively. Hydrogen, carbon, oxygen, and sulfur atoms are represented by white, gray, red, and yellow spheres, respectively.

Related discussions

The -COOH group of GA and -S=O from SO_3 can form six-membered ring in transition state rather than closed four-membered ring. Meanwhile, according to the Electrostatic potential (ESP) on molecular van der Waals (vdW) surface of GA and SO_3 molecules from our previous study,[6] the sulfur atom in the SO_3 molecule possesses more positive ESP and the oxygen atoms of -COOH/-OH group possesses more negative ESP, making both of the two pathways for GA-SO_3 reaction feasible to occur. Also, the oxygen atoms of SO_3 molecule possess relatively negative ESP, which could interact with the hydrogen atoms of -COOH/-OH group. Therefore, the gas-phase reaction between GA and SO_3 is feasible to occur. Furthermore, the SO_3-H_2O reaction, which is commonly recognized as important loss process of SO_3, could be catalyzed by GA. Although H_2O will be dominant sink pathway for SO_3, GA-SO_3 can be comparable to that of SO_3-H_2O in highly polluted areas with relatively dry and cold conditions. The gaseous concentration of H_2O is drastically reduced at lower temperature and dry condition.[7] Hence, the GA-SO_3 reaction may compete with the hydration reaction of SO_3.

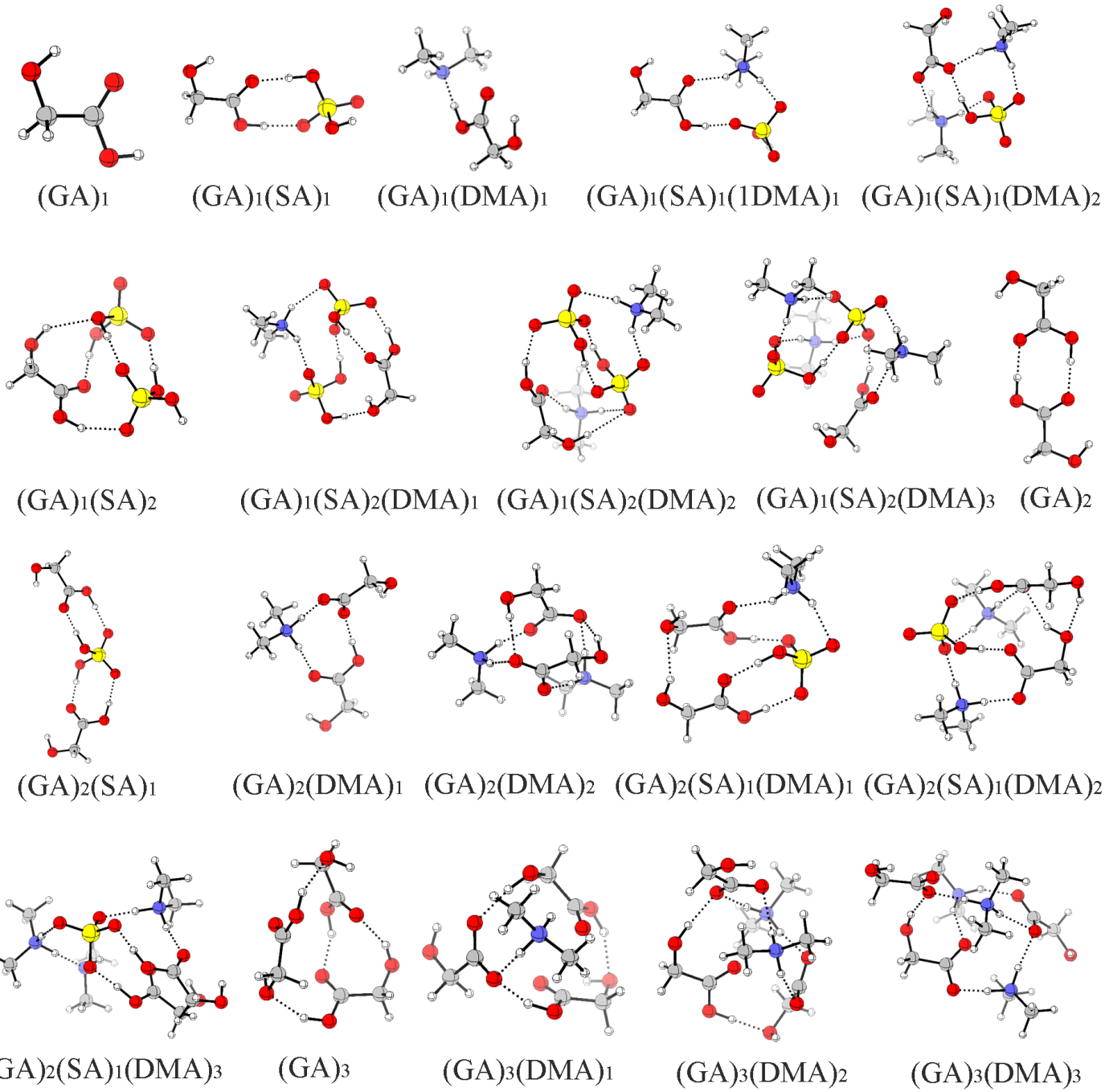

Figure S2. Identified lowest free energy structures of the $(GA)_x(SA)_y(DMA)_z$ ($0 \le z \le x + y \le 3$) clusters at the DLPNO-CCSD(T)/aug-cc-pVTZ//M06-2X/6-311++G(3df,3pd) level of theory. The white, gray, red, and yellow balls represent hydrogen, carbon, oxygen, and sulfur atoms, respectively. Dashed black lines indicate hydrogen bonds.

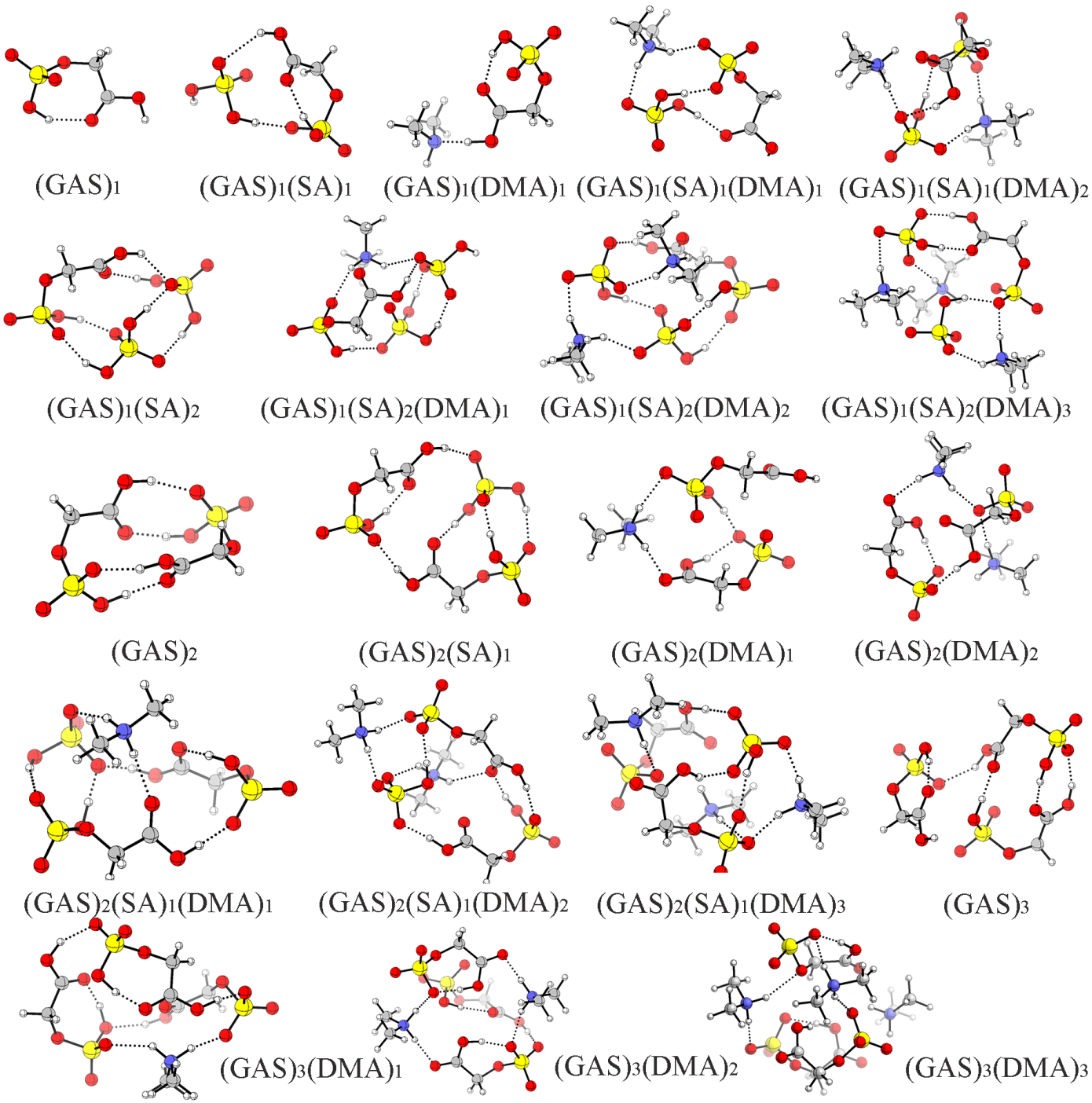

Figure S3. Identified lowest free energy structures of the $(GAS)_x(SA)_y(DMA)_z$ ($0 \le z \le x + y \le 3$) clusters at the DLPNO-CCSD(T)/aug-cc-pVTZ//M06-2X/6-311++G(3df,3pd) level of theory. The white, gray, red, and yellow balls represent hydrogen, carbon, oxygen, and sulfur atoms, respectively. Dashed black lines indicate hydrogen bonds.

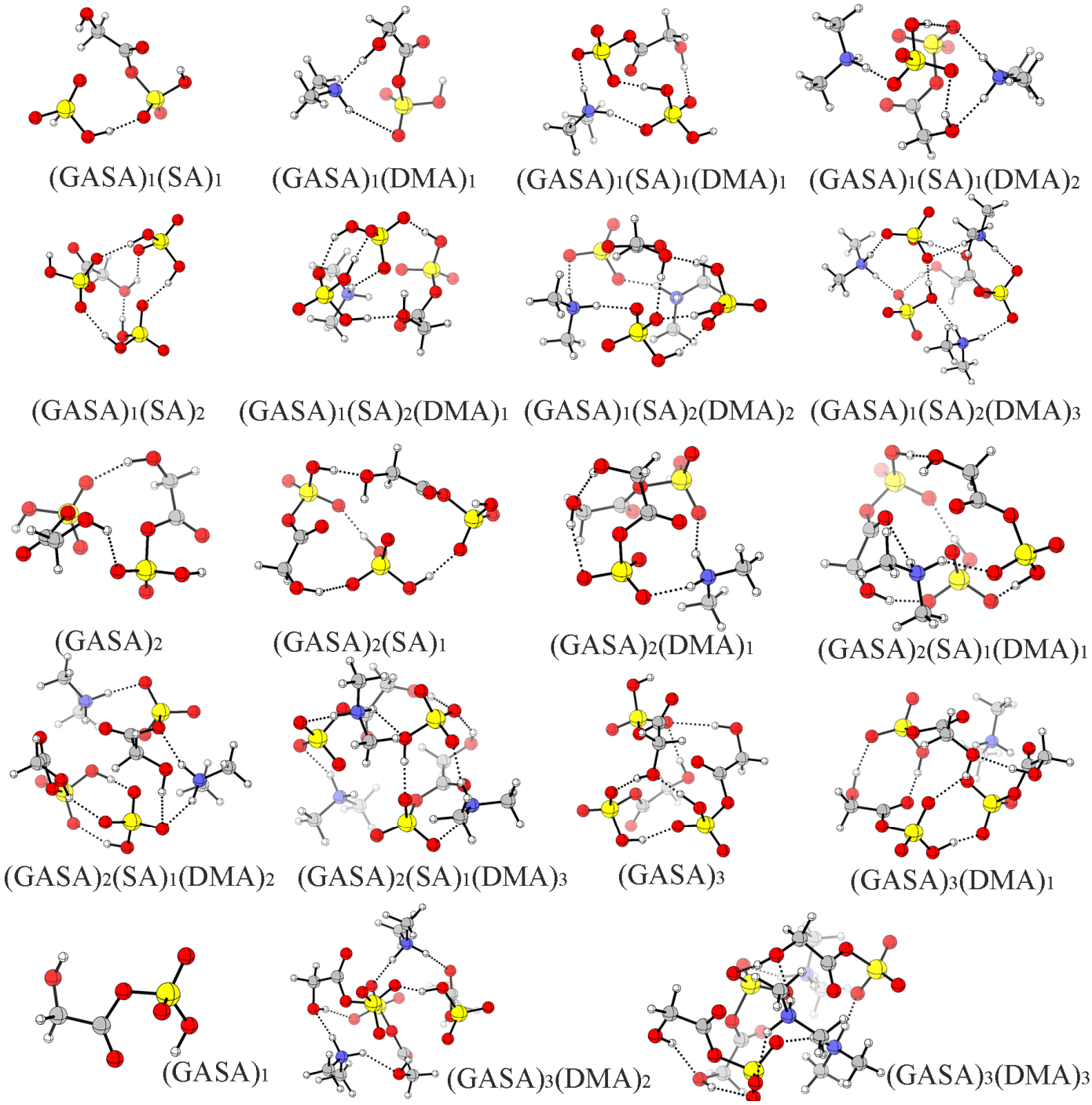

Figure S4. Identified lowest free energy structures of the $(GASA)_x(SA)_y(DMA)_z$ ($0 \le z \le x + y \le 3$) clusters at the DLPNO-CCSD(T)/aug-cc-pVTZ//M06-2X/6-311++G(3df,3pd) level of theory. The white, gray, red, and yellow balls represent hydrogen, carbon, oxygen, and sulfur atoms, respectively. Dashed black lines indicate hydrogen bonds.

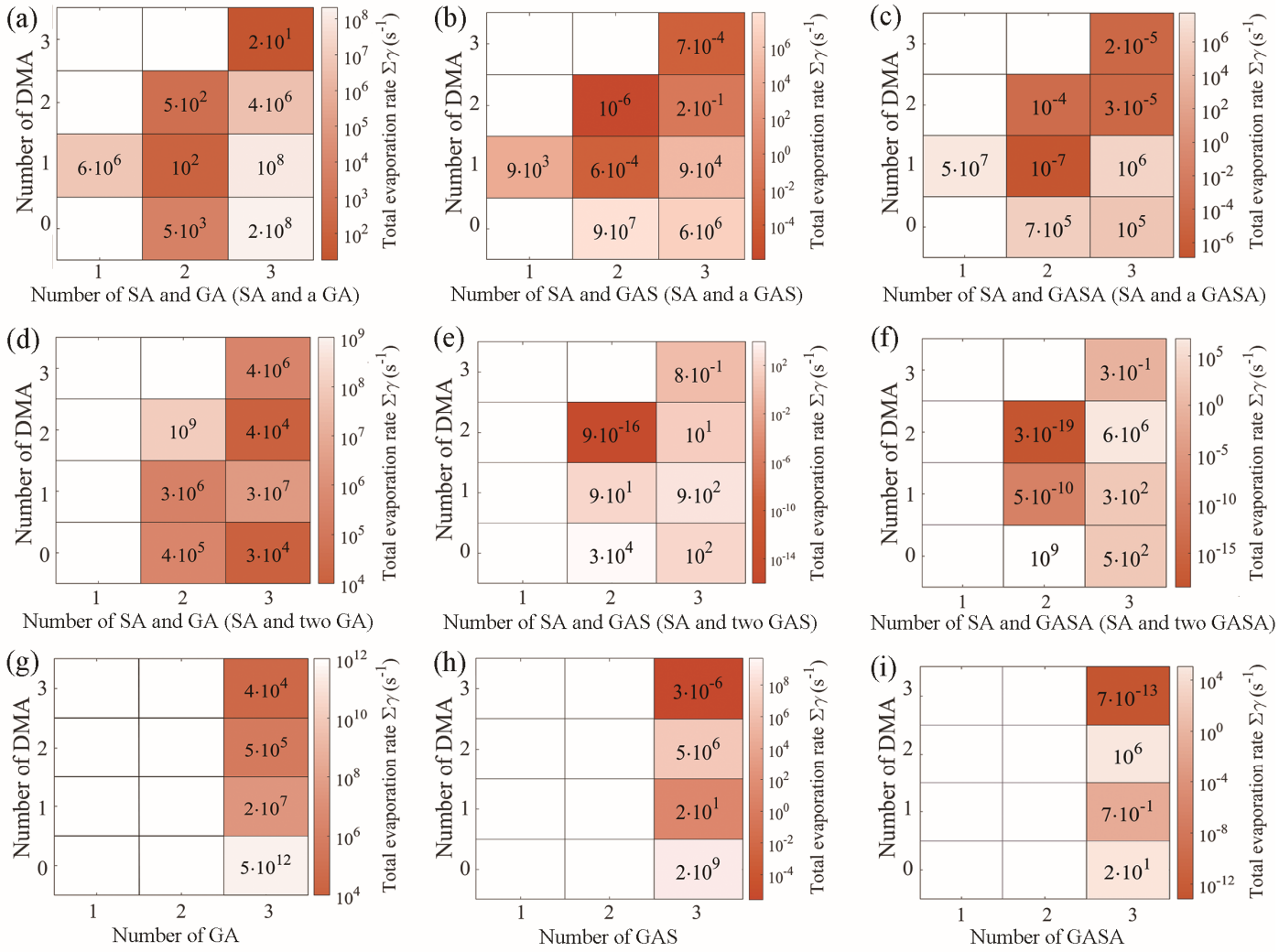

Figure S5. The evaporation rates of $(GA)_x(SA)_y(DMA)_z$ clusters ($1 \le z \le x + y \le 3$) (a, d, g; left panel), $(GAS)_x(SA)_y(DMA)_z$ clusters ($1 \le z \le x + y \le 3$) (b, e, h; center panel), and $(GASA)_x(SA)_y(DMA)_z$ clusters ($1 \le z \le x + y \le 3$) (c, f, i; right panel) at 278 K.

Related discussions

The evaporation rates of the clusters in the GA-SA-DMA system, GAS-SA-DMA system and the GASA-SA-DMA system at 278 K are shown in Figure S5. As can be seen in Figure S5, the evaporation rates for the GA-SA-DMA clusters ($(GA)_1(SA)_1(DMA)_2$, $(GA)_1(SA)_2(DMA)_3$, $(GA)_2(DMA)_2$, $(GA)_2(SA)_1(DMA)_3$, $(GA)_3(DMA)_3$) along the diagonal line of the grid are much higher than those of corresponding GAS-SA-DMA and GASA-SA-DMA clusters, with a range from 10^1 to 10^9 s^{-1} in comparison to those of 10^{-1} to 10^{-19} s^{-1}. Furthermore, the evaporation of one DMA molecule or DMA involved small clusters (such as $(GA)_1(DMA)_1$, $(SA)_1(DMA)_1$, $(GAS)_1(DMA)_1$) was the main degradation pathway for clusters with the equal number of

acidic and base molecules, whereas the acidic monomer evaporation is dominant for clusters, in which the number of acidic molecules (GA, GAS, GASA and SA) is more than that of base molecules (DMA) (Table S3). Generally, clusters with low evaporation rates ($\leqslant 10^{-4}$ s^{-1}) can be deemed as stable against evaporation, and most of the GAS-SA-DMA as well as GASA-SA-DMA clusters have lower evaporation rates than the corresponding GA-SA-DMA clusters, suggesting that the products (GAS/GASA)-involved clusters are more stable than the reactant (GA)-involved clusters. Therefore, we can conclude that GAS/GASA can form more stable clusters with SA-DMA than GA at the same size of acid and base molecules within all of the considered clusters.

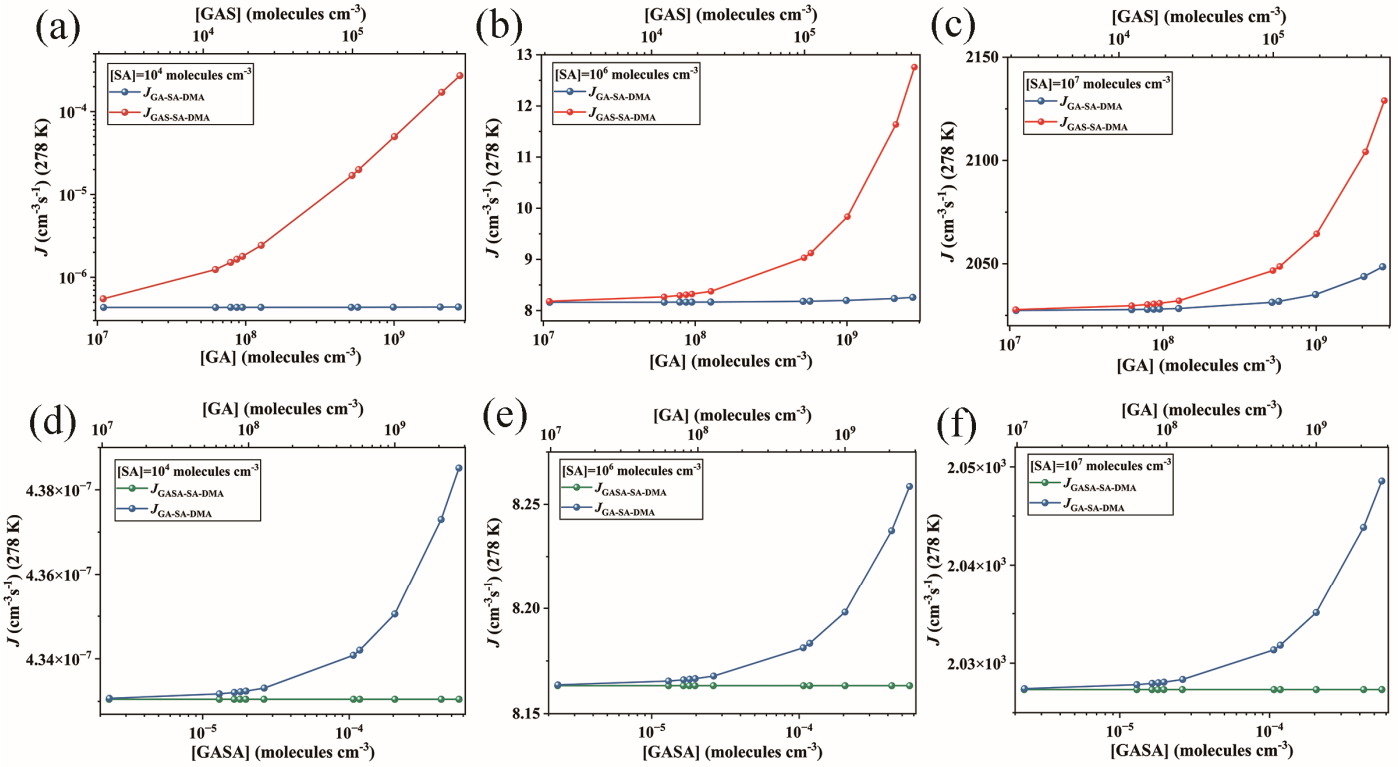

Figure S6. Simulated cluster formation rates J ($cm^{-3}s^{-1}$) as a function of monomer concentrations ([GA], [GAS], and [GASA], respectively) under different [SA] (a) (d) [SA] = 10^4, (b) (e) [SA] = 10^6, and (c) (f) [SA] = 10^7 molecules cm^{-3} at 278 K, [DMA] = 10^8 molecules cm^{-3}.

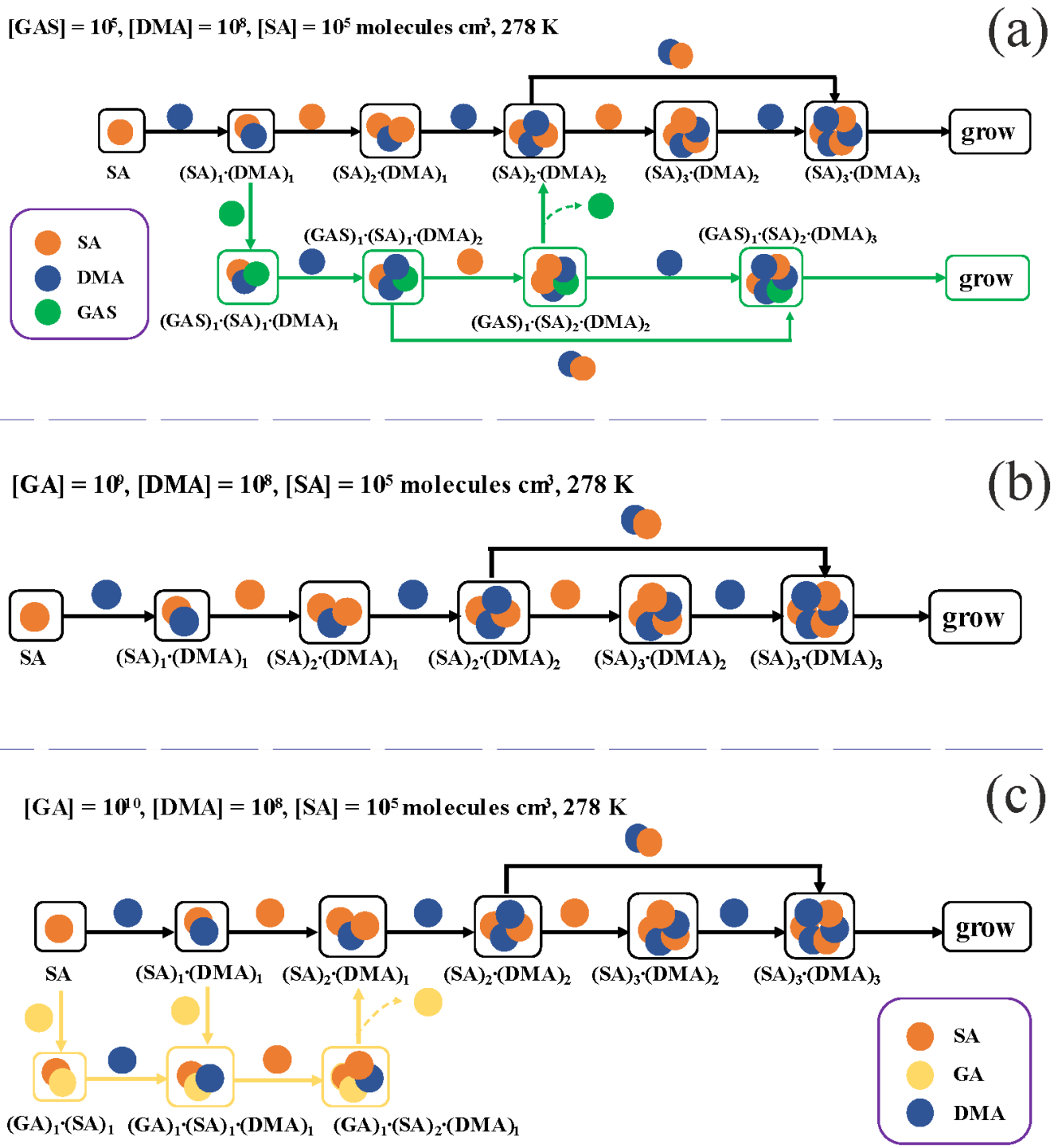

Figure S7. Main cluster growth pathway of (a) GAS-SA-DMA, and (b) (c) GA-SA-DMA nucleating system at 278 K, [DMA] = 10^8, [SA] = 10^5, [GAS] = 10^5 and [GA] = 10^9, 10^{10} molecules cm^{-3}, respectively. The black,green, and light orange arrows refer to the pathways of SA-DMA, GAS-SA-DMA and GA-SA-DMA, respectively.

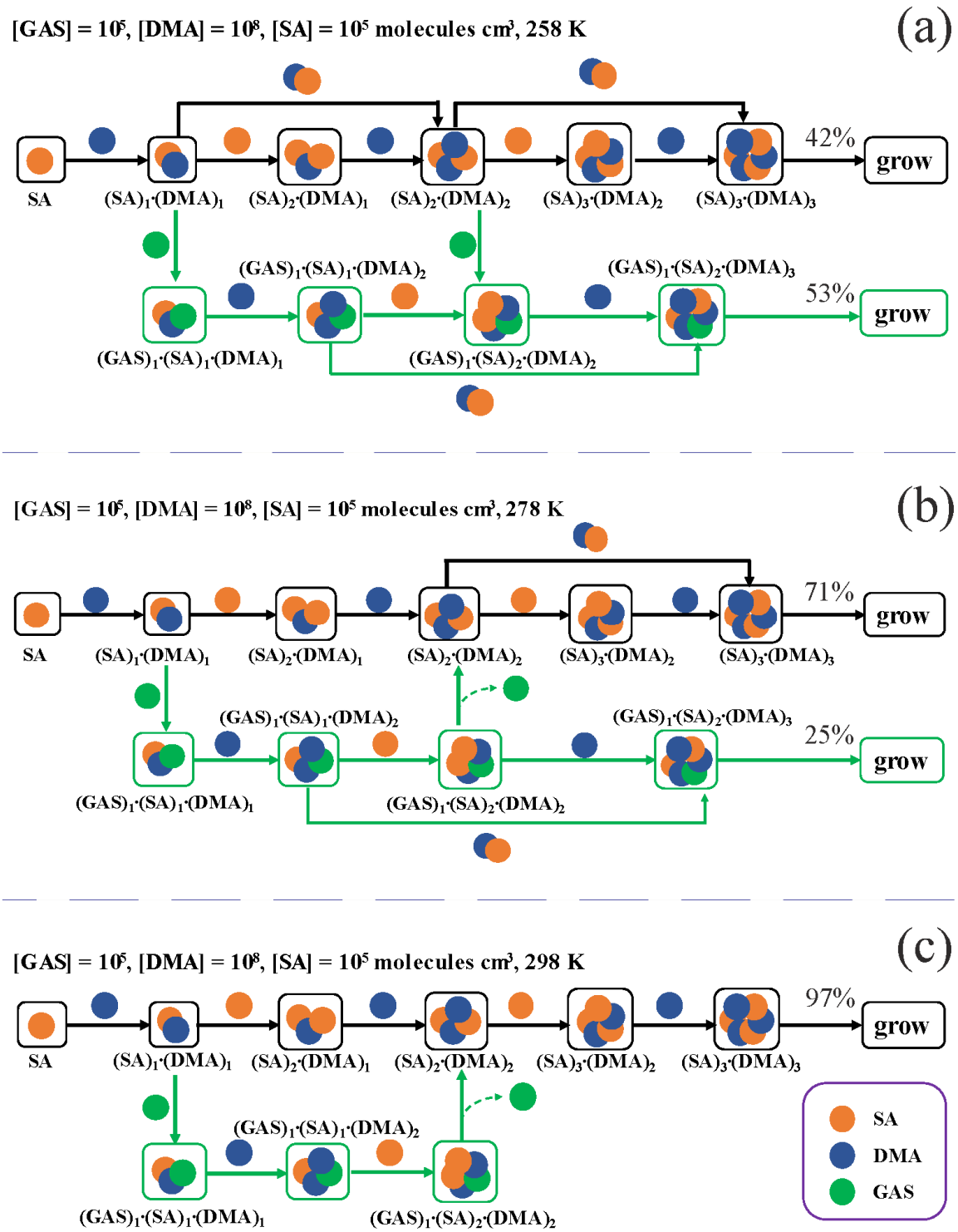

Figure S8. Main cluster growth pathway of GAS-SA-DMA nucleating system at [GAS] = 10^5, [DMA] = 10^8, [SA] = 10^5 molecules cm^{-3}, and (a) 258 K (b) 278 K (c) 298 K. The black and green arrows refer to the pathways of SA-DMA and GAS-SA-DMA, respectively. For clarity, other pathways that contributes less than 5% to the cluster growing out of the studied system are not shown.

Table S1 Equilibrium constants K_{eq} for pathway (1) $(GA + SO_3)_{-OH} \rightarrow GAS$ and pathway (2) $(GA + SO_3)_{-COOH} \rightarrow GASA$ and possible concentrations of GAS and GASA in the atmosphere, based on the formation Gibbs free energy (ΔG) at the DLPNO-CCSD(T)/aug-cc-pVTZ//M06-2X/6-311++G(3df,3pd) level of theory and 278 K, 101.3 KPa.

Reaction pathways	**ΔG (kcal mol^{-1})**	**[GA] (molecules cm^{-3})**	**[SO_3] (molecules cm^{-3})**	**K_{eq} (cm^3 molecule^{-1})**	**[C] (molecules cm^{-3})**
$(GA + SO_3)_{-OH} \rightarrow$ GAS	-13.62	1.11×10^7-2.72×10^9	10^5	1.93×10^{-9}	2.14×10^3-5.24×10^5
$(GA + SO_3)_{-COOH} \rightarrow$ GASA	-2.21	1.11×10^7-2.72×10^9	10^5	2.07×10^{-18}	2.30×10^{-6}-5.62×10^{-4}

Table S2. Calculated Gibbs free energy changes (ΔG) of the formation of heterotrimers consisting of H_2SO_4, base (ammonia/DMA), and GA/GAS/GASA at the temperature of 278 K and pressure of 101.3 KPa.

clusters	ΔG (kcal mol^{-1}) GA-SA-ammonia [a]	ΔG (kcal mol^{-1}) GA-SA-DMA	ΔG (kcal mol^{-1}) GAS-SA-DMA	ΔG (kcal mol^{-1}) GASA-SA-DMA
Org-base	-2.74	-4.23	-7.83	-3.06
Org-SA	-7.55	-7.97	-2.58	-5.27
Org-SA-base	-14.90	-23.12	-29.90	-34.54
Org-SA-2base	-16.68	-32.66	-50.48	-52.57
Org-2SA	-14.55	-11.70	-13.58	-15.75
Org-2SA-base	-28.21	-37.71	-41.62	-40.26
Org-2SA-2base	-36.81	-55.95	-65.39	-71.31
Org-2SA-3base	-41.21	-67.68	-82.56	-90.30
2Org	-5.37	-5.17	-6.68	-0.77
2Org-base	-4.33	-10.05	-18.20	-27.65
2Org-2base	-2.35	-11.59	-50.36	-64.19
2Org-SA	-14.87	-15.04	-16.86	-14.54
2Org-SA-base	-19.96	-26.48	-38.94	-44.23
2Org-SA-2base	-20.99	-39.72	-62.20	-68.50
2Org-SA-3base	-23.42	-44.48	-76.48	-90.80
3Org	-5.24	-1.81	-7.71	-11.82
3Org-base	-6.87	-13.61	-29.49	-40.64
3Org-2base	-6.98	-20.11	-54.73	-69.36
3Org-3base	-3.20	-27.43	-78.18	-98.00

a The data is from J. Chem. Phys. 146, 184308 (2017) "The enhancement mechanism of glycolic acid on the formation of atmospheric sulfuric acid–ammonia molecular clusters" calculated at the level of M06-2X/6-311++G(3df,3pd)//CCSD(T)-F12/VDZ-F12[8].

Table S3. Evaporation rate coefficients (s^{-1}) for simulated evaporation pathways of GA-involved, GAS-involved and GASA-involved clusters at 278 K and 101.3 KPa obtained by the ACDC simulations.

Evaporation pathways	Evaporation rate coefficients
$(SA)_2 \rightarrow SA + SA$	1.40×10^{2}
$(SA)_3 \rightarrow (SA)_2 + SA$	1.01×10^{5}
$(SA)_1(DMA)_1 \rightarrow DMA + SA$	7.46×10^{-1}
$(SA)_2(DMA)_1 \rightarrow (SA)_1(DMA)_1 + SA$	3.92×10^{-8}
$(SA)_2(DMA)_1 \rightarrow DMA + (SA)_2$	9.95×10^{-11}
$(SA)_3(DMA)_1 \rightarrow (SA)_2(DMA)_1 + SA$	7.15×10^{-1}
$(SA)_3(DMA)_1 \rightarrow (SA)_1(DMA)_1 + (SA)_2$	8.07×10^{-11}
$(SA)_3(DMA)_1 \rightarrow DMA + (SA)_3$	6.80×10^{-16}
$(SA)_2(DMA)_2 \rightarrow (SA)_2(DMA)_1 + DMA$	2.32×10^{-3}
$(SA)_2(DMA)_2 \rightarrow (SA)_1(DMA)_1 + (SA)_1(DMA)_1$	5.15×10^{-11}
$(SA)_3(DMA)_2 \rightarrow (SA)_2(DMA)_2 + SA$	2.11×10^{-4}
$(SA)_3(DMA)_2 \rightarrow (SA)_3(DMA)_1 + DMA$	6.66×10^{-7}
$(SA)_3(DMA)_2 \rightarrow (SA)_2(DMA)_1 + (SA)_1(DMA)_1$	4.78×10^{-7}
$(SA)_3(DMA)_3 \rightarrow (SA)_3(DMA)_2 + DMA$	6.58×10^{-4}
$(SA)_3(DMA)_3 \rightarrow (SA)_2(DMA)_2 + (SA)_1(DMA)_1$	1.24×10^{-7}
$(SA)_1(GA)_1 \rightarrow GA + SA$	5.09×10^{3}
$(SA)_2(GA)_1 \rightarrow (SA)_1(GA)_1 + SA$	1.19×10^{7}
$(SA)_2(GA)_1 \rightarrow GA + (SA)_2$	1.94×10^{8}
$(GA)_2 \rightarrow GA + GA$	4.11×10^{5}
$(SA)_1(GA)_2 \rightarrow (GA)_2 + SA$	1.91×10^{2}
$(SA)_1(GA)_2 \rightarrow (SA)_1(GA)_1 + GA$	2.81×10^{4}
$(GA)_3 \rightarrow (GA)_2 + GA$	4.58×10^{12}
$(GA)_1(DMA)_1 \rightarrow GA + DMA$	6.23×10^{6}
$(SA)_1(GA)_1(DMA)_1 \rightarrow (GA)_1(DMA)_1 + SA$	1.55×10^{-5}
$(SA)_1(GA)_1(DMA)_1 \rightarrow (SA)_1(GA)_1 + DMA$	1.83×10^{-2}

$(SA)_1(GA)_1(DMA)_1 \rightarrow GA + (SA)_1(DMA)_1$	1.17×10^{2}
$(SA)_2(GA)_1(DMA)_1 \rightarrow (SA)_1(GA)_1(DMA)_1 + SA$	3.98×10^{-2}
$(SA)_2(GA)_1(DMA)_1 \rightarrow (GA)_1(DMA)_1 + (SA)_2$	1.65×10^{-9}
$(SA)_2(GA)_1(DMA)_1 \rightarrow (SA)_2(GA)_1 + DMA$	5.91×10^{-11}
$(SA)_2(GA)_1(DMA)_1 \rightarrow (SA)_1(GA)_1 + (SA)_1(DMA)_1$	7.66×10^{-4}
$(SA)_2(GA)_1(DMA)_1 \rightarrow GA + (SA)_2(DMA)_1$	1.10×10^{8}
$(GA)_2(DMA)_1 \rightarrow (GA)_2 + DMA$	2.32×10^{6}
$(GA)_2(DMA)_1 \rightarrow (GA)_1(DMA)_1 + GA$	2.90×10^{5}
$(SA)_1(GA)_2(DMA)_1 \rightarrow (GA)_2(DMA)_1 + SA$	1.48×10^{-3}
$(SA)_1(GA)_2(DMA)_1 \rightarrow (SA)_1(GA)_2 + DMA$	1.75×10^{1}
$(SA)_1(GA)_2(DMA)_1 \rightarrow (GA)_2 + (SA)_1(DMA)_1$	3.38×10^{3}
$(SA)_1(GA)_2(DMA)_1 \rightarrow (SA)_1(GA)_1(DMA)_1 + GA$	2.59×10^{7}
$(SA)_1(GA)_2(DMA)_1 \rightarrow (GA)_1(DMA)_1 + (SA)_1(GA)_1$	6.62×10^{-2}
$(GA)_3(DMA)_1 \rightarrow (GA)_3 + DMA$	9.61×10^{0}
$(GA)_3(DMA)_1 \rightarrow (GA)_2(DMA)_1 + GA$	1.83×10^{7}
$(GA)_3(DMA)_1 \rightarrow (GA)_1(DMA)_1 + (GA)_2$	5.59×10^{6}
$(SA)_1(GA)_1(DMA)_2 \rightarrow (SA)_1(GA)_1(DMA)_1 + DMA$	5.40×10^{2}
$(SA)_1(GA)_1(DMA)_2 \rightarrow (GA)_1(DMA)_1 + (SA)_1(DMA)_1$	8.83×10^{-3}
$(SA)_2(GA)_1(DMA)_2 \rightarrow (SA)_1(GA)_1(DMA)_2 + SA$	6.42×10^{-9}
$(SA)_2(GA)_1(DMA)_2 \rightarrow (SA)_2(GA)_1(DMA)_1 + (DMA)_1$	8.50×10^{-5}
$(SA)_2(GA)_1(DMA)_2 \rightarrow (SA)_1(GA)_1(DMA)_1 + (SA)_1(DMA)_1$	3.21×10^{-6}
$(SA)_2(GA)_1(DMA)_2 \rightarrow (GA)_1(DMA)_1 + (SA)_2(DMA)_1$	1.18×10^{-3}
$(SA)_2(GA)_1(DMA)_2 \rightarrow GA + (SA)_2(DMA)_2$	3.90×10^{6}
$(GA)_2(DMA)_2 \rightarrow (GA)_2(DMA)_1 + DMA$	1.11×10^{9}
$(GA)_2(DMA)_2 \rightarrow (GA)_1(DMA)_1 + (GA)_1(DMA)_1$	2.11×10^{7}
$(SA)_1(GA)_2(DMA)_2 \rightarrow (GA)_2(DMA)_2 + SA$	1.04×10^{-12}
$(SA)_1(GA)_2(DMA)_2 \rightarrow (SA)_1(GA)_2(DMA)_1 + DMA$	7.60×10^{-1}
$(SA)_1(GA)_2(DMA)_2 \rightarrow (GA)_2(DMA)_1 + (SA)_1(DMA)_1$	1.01×10^{-3}
$(SA)_1(GA)_2(DMA)_2 \rightarrow (SA)_1(GA)_1(DMA)_2 + GA$	3.53×10^{4}

$(SA)_1(GA)_2(DMA)_2 \rightarrow (SA)_1(GA)_1(DMA)_1 + (GA)_1(DMA)_1$	2.35×10^{0}
$(GA)_3(DMA)_2 \rightarrow (GA)_3(DMA)_1 + DMA$	1.58×10^{5}
$(GA)_3(DMA)_2 \rightarrow (GA)_2(DMA)_2 + GA$	2.54×10^{3}
$(GA)_3(DMA)_2 \rightarrow (GA)_2(DMA)_1 + (GA)_1(DMA)_1$	3.30×10^{5}
$(SA)_2(GA)_1(DMA)_3 \rightarrow (SA)_2(GA)_1(DMA)_2 + DMA$	1.23×10^{1}
$(SA)_2(GA)_1(DMA)_3 \rightarrow (SA)_1(GA)_1(DMA)_2 + (SA)_1(DMA)_1$	6.72×10^{-8}
$(SA)_2(GA)_1(DMA)_3 \rightarrow (GA)_1(DMA)_1 + (SA)_2(DMA)_2$	5.45×10^{0}
$(SA)_1(GA)_2(DMA)_3 \rightarrow (SA)_1(GA)_2(DMA)_2 + DMA$	3.78×10^{6}
$(SA)_1(GA)_2(DMA)_3 \rightarrow (GA)_2(DMA)_2 + (SA)_1(DMA)_1$	3.19×10^{-6}
$(SA)_1(GA)_2(DMA)_3 \rightarrow (SA)_1(GA)_1(DMA)_2 + (GA)_1(DMA)_1$	1.45×10^{4}
$(GA)_3(DMA)_3 \rightarrow (GA)_3(DMA)_2 + DMA$	3.75×10^{4}
$(GA)_3(DMA)_3 \rightarrow (GA)_2(DMA)_2 + (GA)_1(DMA)_1$	9.97×10^{0}
$(SA)_1(GAS)_1 \rightarrow GAS + SA$	8.70×10^{7}
$(SA)_2(GAS)_1 \rightarrow (SA)_1(GAS)_1 + SA$	2.34×10^{1}
$(SA)_2(GAS)_1 \rightarrow GAS + (SA)_2$	6.50×10^{6}
$(GAS)_2 \rightarrow GAS + GAS$	2.65×10^{4}
$(SA)_1(GAS)_2 \rightarrow (GAS)_2 + SA$	1.08×10^{2}
$(SA)_1(GAS)_2 \rightarrow (SA)_1(GAS)_1 + GAS$	5.99×10^{-2}
$(GAS)_3 \rightarrow (GAS)_2 + GAS$	1.64×10^{9}
$(GAS)_1(DMA)_1 \rightarrow GAS + DMA$	9.21×10^{3}
$(SA)_1(GAS)_1(DMA)_1 \rightarrow (GAS)_1(DMA)_1 + SA$	4.96×10^{-8}
$(SA)_1(GAS)_1(DMA)_1 \rightarrow (SA)_1(GAS)_1 + DMA$	5.04×10^{-12}
$(SA)_1(GAS)_1(DMA)_1 \rightarrow GAS + (SA)_1(DMA)_1$	5.51×10^{-4}
$(SA)_2(GAS)_1(DMA)_1 \rightarrow (SA)_1(GAS)_1(DMA)_1 + SA$	7.18×10^{0}
$(SA)_2(GAS)_1(DMA)_1 \rightarrow (GAS)_1(DMA)_1 + (SA)_2$	9.51×10^{-10}
$(SA)_2(GAS)_1(DMA)_1 \rightarrow (SA)_2(GAS)_1 + DMA$	1.50×10^{-12}
$(SA)_2(GAS)_1(DMA)_1 \rightarrow (SA)_1(GAS)_1 + (SA)_1(DMA)_1$	3.81×10^{-11}
$(SA)_2(GAS)_1(DMA)_1 \rightarrow GAS + (SA)_2(DMA)_1$	9.37×10^{4}
$(GAS)_2(DMA)_1 \rightarrow (GAS)_2 + DMA$	1.42×10^{1}

$(GAS)_2(DMA)_1 \rightarrow (GAS)_1(DMA)_1 + GAS$	7.72×10^{1}
$(SA)_1(GAS)_2(DMA)_1 \rightarrow (GAS)_2(DMA)_1 + SA$	6.08×10^{-7}
$(SA)_1(GAS)_2(DMA)_1 \rightarrow (SA)_1(GAS)_2 + DMA$	7.76×10^{-8}
$(SA)_1(GAS)_2(DMA)_1 \rightarrow (GAS)_2 + (SA)_1(DMA)_1$	8.48×10^{-6}
$(SA)_1(GAS)_2(DMA)_1 \rightarrow (SA)_1(GAS)_1(DMA)_1 + GAS$	8.86×10^{2}
$(SA)_1(GAS)_2(DMA)_1 \rightarrow (GAS)_1(DMA)_1 + (SA)_1(GAS)_1$	4.24×10^{-13}
$(GAS)_3(DMA)_1 \rightarrow (GAS)_3 + DMA$	1.39×10^{-7}
$(GAS)_3(DMA)_1 \rightarrow (GAS)_2(DMA)_1 + GAS$	1.55×10^{1}
$(GAS)_3(DMA)_1 \rightarrow (GAS)_1(DMA)_1 + (GAS)_2$	1.95×10^{-2}
$(SA)_1(GAS)_1(DMA)_2 \rightarrow (SA)_1(GAS)_1(DMA)_1 + DMA$	1.13×10^{-6}
$(SA)_1(GAS)_1(DMA)_2 \rightarrow (GAS)_1(DMA)_1 + (SA)_1(DMA)_1$	5.90×10^{-14}
$(SA)_2(GAS)_1(DMA)_2 \rightarrow (SA)_1(GAS)_1(DMA)_2 + SA$	2.47×10^{-2}
$(SA)_2(GAS)_1(DMA)_2 \rightarrow (SA)_2(GAS)_1(DMA)_1 + DMA$	3.80×10^{-9}
$(SA)_2(GAS)_1(DMA)_2 \rightarrow (SA)_1(GAS)_1(DMA)_1 + (SA)_1(DMA)_1$	2.58×10^{-8}
$(SA)_2(GAS)_1(DMA)_2 \rightarrow (GAS)_1(DMA)_1 + (SA)_2(DMA)_1$	3.04×10^{-8}
$(SA)_2(GAS)_1(DMA)_2 \rightarrow GAS + (SA)_2(DMA)_2$	1.48×10^{-1}
$(GAS)_2(DMA)_2 \rightarrow (GAS)_2(DMA)_1 + DMA$	9.33×10^{-16}
$(GAS)_2(DMA)_2 \rightarrow (GAS)_1(DMA)_1 + (GAS)_1(DMA)_1$	3.20×10^{-18}
$(SA)_1(GAS)_2(DMA)_2 \rightarrow (GAS)_2(DMA)_2 + SA$	6.61×10^{0}
$(SA)_1(GAS)_2(DMA)_2 \rightarrow (SA)_1(GAS)_2(DMA)_1 + DMA$	9.94×10^{-9}
$(SA)_1(GAS)_2(DMA)_2 \rightarrow (GAS)_2(DMA)_1 + (SA)_1(DMA)_1$	5.42×10^{-15}
$(SA)_1(GAS)_2(DMA)_2 \rightarrow (SA)_1(GAS)_1(DMA)_2 + GAS$	7.56×10^{0}
$(SA)_1(GAS)_2(DMA)_2 \rightarrow (SA)_1(GAS)_1(DMA)_1 + (GAS)_1(DMA)_1$	7.13×10^{-10}
$(GAS)_3(DMA)_2 \rightarrow (GAS)_3(DMA)_1 + DMA$	2.85×10^{-10}
$(GAS)_3(DMA)_2 \rightarrow (GAS)_2(DMA)_2 + GAS$	4.62×10^{6}
$(GAS)_3(DMA)_2 \rightarrow (GAS)_2(DMA)_1 + (GAS)_1(DMA)_1$	3.24×10^{-13}
$(SA)_2(GAS)_1(DMA)_3 \rightarrow (SA)_2(GAS)_1(DMA)_2 + DMA$	6.38×10^{-4}
$(SA)_2(GAS)_1(DMA)_3 \rightarrow (SA)_1(GAS)_1(DMA)_2 + (SA)_1(DMA)_1$	1.34×10^{-5}
$(SA)_2(GAS)_1(DMA)_3 \rightarrow (GAS)_1(DMA)_1 + (SA)_2(DMA)_2$	7.27×10^{-9}

$(SA)_1(GAS)_2(DMA)_3 \rightarrow (SA)_1(GAS)_2(DMA)_2 + DMA$	1.23×10^{-1}
$(SA)_1(GAS)_2(DMA)_3 \rightarrow (GAS)_2(DMA)_2 + (SA)_1(DMA)_1$	6.65×10^{-1}
$(SA)_1(GAS)_2(DMA)_3 \rightarrow (SA)_1(GAS)_1(DMA)_2 + (GAS)_1(DMA)_1$	6.86×10^{-5}
$(GAS)_3(DMA)_3 \rightarrow (GAS)_3(DMA)_2 + DMA$	7.91×10^{-9}
$(GAS)_3(DMA)_3 \rightarrow (GAS)_2(DMA)_2 + (GAS)_1(DMA)_1$	2.58×10^{-6}
$(SA)_1(GASA)_1 \rightarrow GASA + SA$	6.74×10^{5}
$(SA)_2(GASA)_1 \rightarrow (SA)_1(GASA)_1 + SA$	5.89×10^{1}
$(SA)_2(GASA)_1 \rightarrow GASA + (SA)_2$	1.27×10^{5}
$(GASA)_2 \rightarrow GASA + GASA$	1.19×10^{9}
$(SA)_1(GASA)_2 \rightarrow (GASA)_2 + SA$	1.62×10^{-1}
$(SA)_1(GASA)_2 \rightarrow (SA)_1(GASA)_1 + GASA$	5.20×10^{2}
$(GASA)_3 \rightarrow (GASA)_2 + GASA$	2.17×10^{1}
$(GASA)_1(DMA)_1 \rightarrow GASA + DMA$	5.14×10^{7}
$(SA)_1(GASA)_1(DMA)_1 \rightarrow (GASA)_1(DMA)_1 + SA$	1.99×10^{-15}
$(SA)_1(GASA)_1(DMA)_1 \rightarrow (SA)_1(GASA)_1 + DMA$	1.46×10^{-13}
$(SA)_1(GASA)_1(DMA)_1 \rightarrow GASA + (SA)_1(DMA)_1$	1.23×10^{-7}
$(SA)_2(GASA)_1(DMA)_1 \rightarrow (SA)_1(GASA)_1(DMA)_1 + SA$	3.77×10^{5}
$(SA)_2(GASA)_1(DMA)_1 \rightarrow (GASA)_1(DMA)_1 + (SA)_2$	2.00×10^{-12}
$(SA)_2(GASA)_1(DMA)_1 \rightarrow (SA)_2(GASA)_1 + DMA$	9.05×10^{-10}
$(SA)_2(GASA)_1(DMA)_1 \rightarrow (SA)_1(GASA)_1 + (SA)_1(DMA)_1$	5.78×10^{-8}
$(SA)_2(GASA)_1(DMA)_1 \rightarrow GASA + (SA)_2(DMA)_1$	1.10×10^{6}
$(GASA)_2(DMA)_1 \rightarrow (GASA)_2 + DMA$	1.16×10^{-11}
$(GASA)_2(DMA)_1 \rightarrow (GASA)_1(DMA)_1 + GASA$	5.09×10^{-10}
$(SA)_1(GASA)_2(DMA)_1 \rightarrow (GASA)_2(DMA)_1 + SA$	1.13×10^{-3}
$(SA)_1(GASA)_2(DMA)_1 \rightarrow (SA)_1(GASA)_2 + DMA$	7.91×10^{-14}
$(SA)_1(GASA)_2(DMA)_1 \rightarrow (GASA)_2 + (SA)_1(DMA)_1$	1.30×10^{-14}
$(SA)_1(GASA)_2(DMA)_1 \rightarrow (SA)_1(GASA)_1(DMA)_1 + GASA$	2.71×10^{2}
$(SA)_1(GASA)_2(DMA)_1 \rightarrow (GASA)_1(DMA)_1 + (SA)_1(GASA)_1$	6.7×10^{-19}
$(GASA)_3(DMA)_1 \rightarrow (GASA)_3 + DMA$	4.00×10^{-13}

$(GASA)_3(DMA)_1 \rightarrow (GASA)_2(DMA)_1 + GASA$	7.19×10^{-1}
$(GASA)_3(DMA)_1 \rightarrow (GASA)_1(DMA)_1 + (GASA)_2$	1.33×10^{-19}
$(SA)_1(GASA)_1(DMA)_2 \rightarrow (SA)_1(GASA)_1(DMA)_1 + DMA$	1.14×10^{-4}
$(SA)_1(GASA)_1(DMA)_2 \rightarrow (GASA)_1(DMA)_1 + (SA)_1(DMA)_1$	2.38×10^{-19}
$(SA)_2(GASA)_1(DMA)_2 \rightarrow (SA)_1(GASA)_1(DMA)_2 + SA$	2.44×10^{-5}
$(SA)_2(GASA)_1(DMA)_2 \rightarrow (SA)_2(GASA)_1(DMA)_1 + DMA$	7.19×10^{-15}
$(SA)_2(GASA)_1(DMA)_2 \rightarrow (SA)_1(GASA)_1(DMA)_1 + (SA)_1(DMA)_1$	2.57×10^{-9}
$(SA)_2(GASA)_1(DMA)_2 \rightarrow (GASA)_1(DMA)_1 + (SA)_2(DMA)_1$	1.21×10^{-16}
$(SA)_2(GASA)_1(DMA)_2 \rightarrow GASA + (SA)_2(DMA)_2$	3.30×10^{-6}
$(GASA)_2(DMA)_2 \rightarrow (GASA)_2(DMA)_1 + DMA$	3.38×10^{-19}
$(GASA)_2(DMA)_2 \rightarrow (GASA)_1(DMA)_1 + (GASA)_1(DMA)_1$	1.37×10^{-36}
$(SA)_1(GASA)_2(DMA)_2 \rightarrow (GASA)_2(DMA)_2 + SA$	5.51×10^{6}
$(SA)_1(GASA)_2(DMA)_2 \rightarrow (SA)_1(GASA)_2(DMA)_1 + DMA$	1.62×10^{-9}
$(SA)_1(GASA)_2(DMA)_2 \rightarrow (GASA)_2(DMA)_1 + (SA)_1(DMA)_1$	1.64×10^{-12}
$(SA)_1(GASA)_2(DMA)_2 \rightarrow (SA)_1(GASA)_1(DMA)_2 + GASA$	3.73×10^{-3}
$(SA)_1(GASA)_2(DMA)_2 \rightarrow (SA)_1(GASA)_1(DMA)_1 + (GASA)_1(DMA)_1$	6.35×10^{-15}
$(GASA)_3(DMA)_2 \rightarrow (GASA)_3(DMA)_1 + DMA$	5.28×10^{-13}
$(GASA)_3(DMA)_2 \rightarrow (GASA)_2(DMA)_2 + GASA$	1.09×10^{6}
$(GASA)_3(DMA)_2 \rightarrow (GASA)_2(DMA)_1 + (GASA)_1(DMA)_1$	5.25×10^{-21}
$(SA)_2(GASA)_1(DMA)_3 \rightarrow (SA)_2(GASA)_1(DMA)_2 + DMA$	2.38×10^{-5}
$(SA)_2(GASA)_1(DMA)_3 \rightarrow (SA)_1(GASA)_1(DMA)_2 + (SA)_1(DMA)_1$	4.92×10^{-10}
$(SA)_2(GASA)_1(DMA)_3 \rightarrow (GASA)_1(DMA)_1 + (SA)_2(DMA)_2$	1.08×10^{-18}
$(SA)_1(GASA)_2(DMA)_3 \rightarrow (SA)_1(GASA)_2(DMA)_2 + DMA$	6.15×10^{-8}
$(SA)_1(GASA)_2(DMA)_3 \rightarrow (GASA)_2(DMA)_2 + (SA)_1(DMA)_1$	2.76×10^{-1}
$(SA)_1(GASA)_2(DMA)_3 \rightarrow (SA)_1(GASA)_1(DMA)_2 + (GASA)_1(DMA)_1$	3.02×10^{-18}
$(GASA)_3(DMA)_3 \rightarrow (GASA)_3(DMA)_2 + DMA$	6.62×10^{-13}
$(GASA)_3(DMA)_3 \rightarrow (GASA)_2(DMA)_2 + (GASA)_1(DMA)_1$	9.16×10^{-15}

166
167

Reference

(1) Mochizuki, T.; Kawamura, K.; Miyazaki, Y.; Kunwar, B.; Boreddy, S. K. R., Distributions and Sources of Low-molecular-weight Monocarboxylic Acids in Gas and Particles from a Deciduous Broadleaf Forest in Northern Japan. *Atmos. Chem. Phys.* **2019,** *19* (4), 2421-2432.

(2) Miyazaki, Y.; Sawano, M.; Kawamura, K., Low-molecular-weight Hydroxyacids in Marine Atmospheric Aerosol: Evidence of a Marine Microbial Origin. *Biogeosciences* **2014,** *11* (16), 4407-4414.

(3) Stieger, B.; van Pinxteren, D.; Tilgner, A.; Spindler, G.; Poulain, L.; Grüner, A.; Wallasch, M.; Herrmann, H., Strong Deviations from Thermodynamically Expected Phase Partitioning of Low-Molecular-Weight Organic Acids during One Year of Rural Measurements. *ACS Earth Space Chem.* **2021,** *5* (3), 500-515.

(4) Mochizuki, T.; Kawamura, K.; Nakamura, S.; Kanaya, Y.; Wang, Z., Enhanced Levels of Atmospheric Low-molecular Weight Monocarboxylic Acids in Gas and Particulates over Mt. Tai, North China, during Field Burning of Agricultural Wastes. *Atmos. Environ.* **2017,** *171*, 237-247.

(5) Liu, L.; Yu, F.; Du, L.; Yang, Z.; Francisco, J. S.; Zhang, X., Rapid Sulfuric Acid–Dimethylamine Nucleation Enhanced by Nitric Acid in Polluted Regions. *Proc. Natl. Acad. Sci. U.S.A.* **2021,** *118* (35), e2108384118.

(6) Tan, S.; Zhang, X.; Lian, Y.; Chen, X.; Yin, S.; Du, L.; Ge, M., OH Group Orientation Leads to Organosulfate Formation at the Liquid Aerosol Surface. *J. Am. Chem. Soc.* **2022,** *144* (37), 16953-16964.

(7) Renard, J. J.; Calidonna, S. E.; Henley, M. V., Fate of ammonia in the atmosphere—a review for applicability to hazardous releases. *J. Hazard. Mater.* **2004,** *108*, (1), 29-60.

(8) Zhang, H.; Kupiainen-Määttä, O.; Zhang, X.; Molinero, V.; Zhang, Y.; Li, Z., The Enhancement Mechanism of Glycolic Acid on the Formation of Atmospheric Sulfuric Acid–ammonia Molecular Clusters. *J. Chem. Phys.* **2017,** *146* (18), 184308.